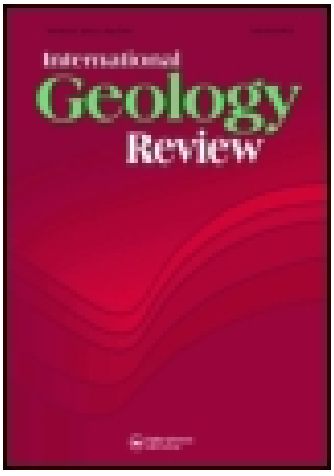

International Geology Review
Publication details, including instructions for authors and subscription information:
http://www.tandfonline.com/loi/tigr20

SHRIMP Zircon U-Pb Age, Geochemistry, and Nd-Sr Isotopes of the Gaojiacun Mafic-Ultramafic Intrusive Complex, Southwest China

W.-G. Zhu [a], H. Zhong [a], H.-L. Deng [a], A. H. Wilson [b], B.-G. Liu [c], C.-Y. Li [a] & Y. Qin [d]

[a] Institute of Geochemistry, Chinese Academy of Sciences

[b] University of Natal

[c] Institute of Geology and Geophysics, Chinese Academy of Sciences

[d] Bureau of Metallurgical Geology and Mineral Exploration

Published online: 06 Aug 2010.

To cite this article: W.-G. Zhu , H. Zhong , H.-L. Deng , A. H. Wilson , B.-G. Liu , C.-Y. Li & Y. Qin (2006) SHRIMP Zircon U-Pb Age, Geochemistry, and Nd-Sr Isotopes of the Gaojiacun Mafic-Ultramafic Intrusive Complex, Southwest China, International Geology Review, 48:7, 650-668

To link to this article: http://dx.doi.org/10.2747/0020-6814.48.7.650

International Geology Review, Vol. 48, 2006, p. 650–668.

SHRIMP Zircon U-Pb Age, Geochemistry, and Nd-Sr Isotopes of the Gaojiacun Mafic-Ultramafic Intrusive Complex, Southwest China

W.-G. ZHU,[1] H. ZHONG, H.-L. DENG,

Key Laboratory of Ore Deposit Geochemistry, Institute of Geochemistry, Chinese Academy of Sciences, 46 Guanshui Road, Guiyang 550002, People's Republic of China

A. H. WILSON,

School of Geological and Computer Sciences, University of Natal, Durban 4041, South Africa

B.-G. LIU,

Institute of Geology and Geophysics, Chinese Academy of Sciences, Beijing 100029, People's Republic of China

C.-Y. LI,

Key Laboratory of Ore Deposit Geochemistry, Institute of Geochemistry, Chinese Academy of Sciences, 46 Guanshui Road, Guiyang 550002, People's Republic of China

AND Y. QIN

Geological Team 601, Bureau of Metallurgical Geology and Mineral Exploration, Panzhihua 617027, People's Republic of China

Abstract

The Gaojiacun mafic-ultramafic intrusive complex in the Yanbian area, Sichuan Province, Southwest China, is a layered intrusive body that underwent intensive magmatic differentiation during two cumulative cycles. SHRIMP (sensitive high-resolution ion microprobe) zircon U-Pb data show that the Gaojiacun complex was formed at 825 ± 12 Ma. These mafic-ultramafic rocks are relatively enriched in light rare-earth elements (LREE) and large-ion lithophile elements (LILE), but are relatively depleted in high-field-strength elements (HFSE). They are characterized by low initial $^{87}Sr/^{86}Sr$ (0.7045 to 0.7050) and positive $\varepsilon_{Nd}(t)$ values (+1.3 to +4.5). The geochemical data indicate that the parental magma of the mafic/ultramafic rocks was derived from a depleted mantle source, and underwent fractional crystallization and crustal contamination. We suggest that the Gaojiacun complex was formed in a continental rift related to mantle superplume activity beneath the Neoproterozoic supercontinent Rodinia.

Introduction

THE EARLY NEOPROTEROZOIC collision between the Yangtze and Cathaysia cratons has been linked to the Neoproterozoic Rodinia reconstruction (Li Z. H. et al., 1995, 1996). U-Pb zircon ages of 0.97 Ga (Zhou G. Q. and Zhao, 1991; Li X. H. et al., 1994; Gan et al., 1996) and Sm-Nd mineral isochron ages of ~1.0 Ga (Zhou X. M. et al., 1989; Chen et al., 1991) for ophiolites from both northeast Jiangxi–southern Anhui and northern Guangxi provinces provide a lower limit on the timing of collision between the Yangtze and Cathaysia cratons. The ophiolites, which are almost coeval with Grenvillian orogenic belts, were considered to signify the final formation of Rodinia in South China. However, the time and mechanism producing the breakup of the supercontinent are still debated. Neoproterozoic magmatic rocks dated at ca. 830–750 Ma have been interpreted as being associated with the breakup of Rodinia. Some researchers have suggested that these Neoproterozoic magmatic rocks were produced by mantle plumes or a super-plume (Li Z. X. et al., 1995, 1996, 1999, 2003; Li X. H. et al., 2002a, 2002b, 2003; Li W. X. et al., 2005; Ling et al., 2003; Wang and Li, 2003). As an alternative view, because all these Neoproterozoic igneous rocks occurred exclusively around the Yangtze craton, with some rocks showing arc-like geochemical

[1]Corresponding author; email: zhuweiguang@vip.gyig.ac.cn

signatures, as well as the occurrence of a ~1.0 Ga ophiolite suite in the SE Yangtze craton, other workers have speculated that active continental margins existed around the Yangtze craton during the Early Neoproterozoic, and that collision between the Yangtze and Cathaysia cratons did not take place until ca. 800 Ma (Shen W. Z. et al., 2002, 2003; Yan et al., 2002; Zhou M. F. et al., 2002a, 2002b; Zhou J. C. et al., 2004). Thus, studies on the timing and tectonic setting of Neoproterozoic magmatic rocks around the Yangtze craton could play an important role in understanding the processes of Neoproterozoic tectonic evolution, and clarify the question of assembly and breakup of supercontinental Rodinia in South China.

Neoproterozoic magmatic rocks are widespread along the western margin of the Yangtze craton. Recent studies indicate that Neoproterozoic magmatism in the western margin of the Yangtze craton corresponds to that in the southern and southeastern margin (Shen W. Z. et al., 2002, 2003; Ling et al., 2003). However, previous studies focused on Neoproterozoic felsic magmatic rocks, with little attention being paid to mafic magmatic rocks (Li X. H. et al., 2002b).

The Gaojiacun intrusive complex, which is located in the Yanbian area, Sichuan Province, Southwest China, is a typical, large mafic/ultramafic intrusive complex exposed along the western margin of the Yangtze craton. Two main hypotheses have been proposed for its origin. One holds that the Gaojiacun complex is part of an ophiolite (Geological Team, 1975; Li J. L. et al., 1983; Luo, 1983; Zhu Z. X., 1983; Shen S. Y. et al., 1986; Sun and Vuagnat, 1992; Sun, 1994). The other suggests that the Gaojiacun complex is an intrusive complex generated in response to Late Mesoproterozoic or Neoproterozoic arc magmatism (Cong, 1988; Shen S. Y. et al., 1986; Shen W. Z. et al., 2003). In this paper, we present SHRIMP zircon U-Pb age, geochemical, and Nd-Sr isotopic data to constrain the age of formation and petrogenesis of the Gaojiacun complex. Thereby we hope to achieve a better understanding of the Neoproterozoic tectonic evolution of the western margin of the Yangtze craton.

Geological History

The Kangding-Panzhihua area is located on the western margin of the Yangtze craton, to the east of the Songpan-Ganzi fold belt (Fig. 1). The basement of the Yangtze craton locally comprises the Archean–Paleoproterozoic Kangding-Tongde complexes, composed of granulite-amphibolite–facies metamorphic rocks, and Mesoproterozoic Huili Group or its equivalents, the Yanbian Group, which consists of metasedimentary rocks interbedded with felsic and mafic metavolcanic rocks. The basement is overlain by a thick sequence (>9 km) of Sinian (610–850 Ma) to Permian strata composed of clastic, carbonate, and metavolcanic rocks. The Lower Sinian Suxiong and Kaijianqiao formations consist of clastic rocks and felsic volcanic rocks, while the Upper Sinian Guanyinya and Dengying Formations consist of clastic rocks in the lower part and phosphorous-bearing carbonate rocks in the upper part (Cong, 1988; SBGMR, 1991). However, SHRIMP zircon U-Pb ages for the Kangding, Miyi, Datian, and Tongde complexes, which were considered to be a part of the Archean–Paleoproterozoic basement, were recently dated at 751–820 Ma (Zhou M. F. et al., 2002b; Li Z. X. et al., 2003).

Neoproterozoic magmatic rocks are widely distributed in the Kangding-Panzhihua area, including granites, granodiorites, tonalites, gabbros, mafic dikes, and small ultramafic bodies (Li Z. X. et al., 1999, 2003; Li X. H. et al., 2002a). These magmatic rocks can be subdivided into two major populations according to their ages. The earlier rocks range in age from ca. 830–820 Ma (Li X. H. et al., 2003). The later rocks mostly have ages of ca. 780–750 Ma (Li Z. X. et al., 2003). Radiometric ages for the Suxiong/Kaijianqiao Formations range from ca. 815 ± 12 Ma (Rb-Sr whole-rock isochron) in the middle-lower part to 803 ± 12 Ma (SHRIMP zircon U-Pb) in the middle-upper part of the succession (Li X. H. et al., 2002a). Ages of the Suxiong/Kaijianqiao formations represent the timing of earlier Neoproterozoic continental basins along the western margin of the Yangtze craton.

Neoproterozoic mafic/ultramafic rocks are mainly located in the Yanbian, Dacao, and Caiziyuan areas on the western margin of the Yangtze craton. In addition, some mafic-ultramafic complexes, mafic dikes, and basalts occurred in the Kangding-Luding-Shimian area, which lies in the northern part in the western margin of the Yangtze craton (Zhu W. G. et al., 2004a).

Geology of the Gaojiacun Mafic-Ultramafic Intrusive Complex

More than 10 intrusive bodies, including the Gaojiacun complex, are exposed in the Yanbian

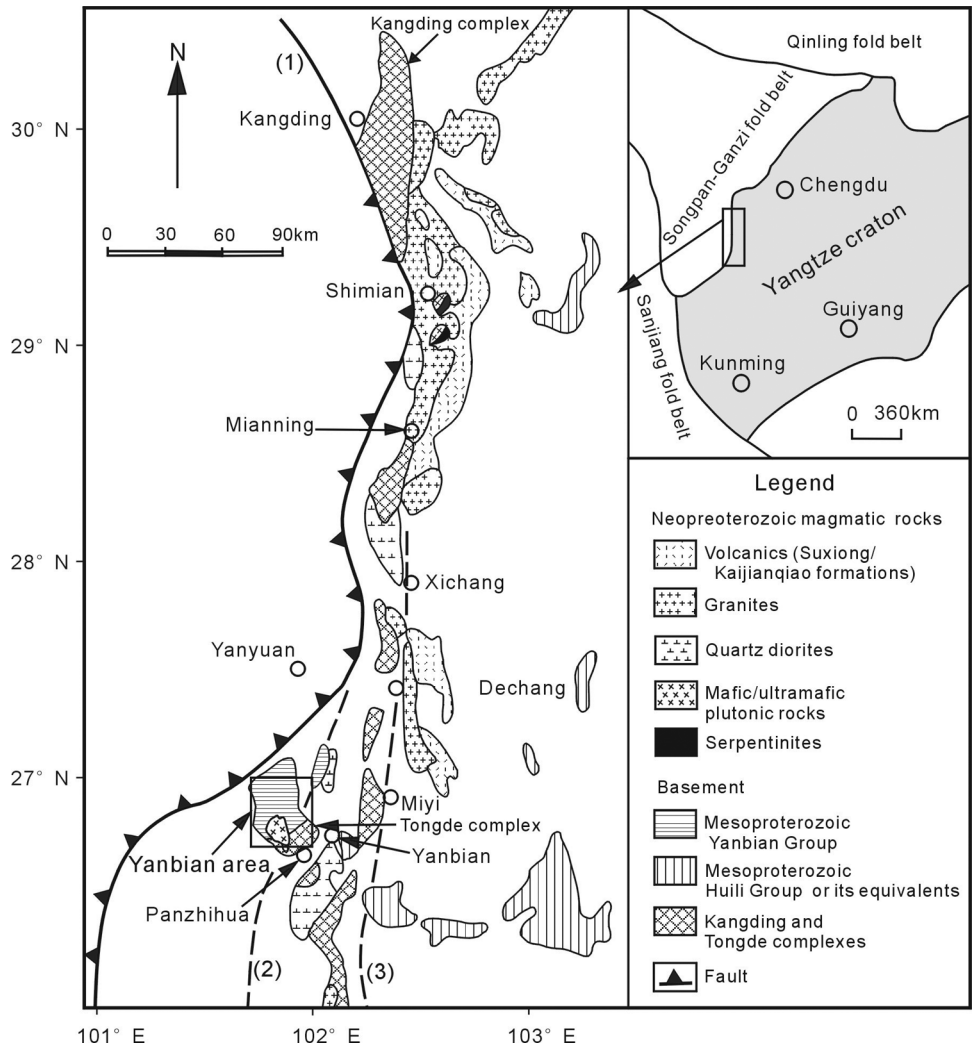

FIG. 1. Simplified geological map of Neoproterozoic magmatic rocks on the western margin of the Yangtze craton (modified after Sun and Vuagnat, 1992). Symbols: 1 = Jinhe-Qinghe fault; 2 = Panzhihua fault; 3 = Xigeda fault.

area, Sichuan Province. The Gaojiacun complex extends northwestward and is irregularly elliptical in shape, measuring 9 km in length and 7.5 km in width, and covering an area of about 70 km^2 (Fig. 2). This complex intruded the metavolcanic rocks and schists of the Mesoproterozoic Yanbian Group. Some small branches of the complex intruded the metavolcanic rocks and schists locally in the contact zone. Brecciaed country-rock xenoliths of different sizes and composition are exposed on the margins of the complex (Shen S. Y. et al., 1986; Cong, 1988). The Lengshuiqing magmatic Cu-Ni sulfide ore deposit is located to the northeast of the complex. The Tongde dioritic complex is exposed to the southeast and southwest.

The Gaojiacun layered intrusion is a well-differentiated mafic-ultramafic intrusive complex consisting of two cumulative cycles (Fig. 3). Cycle I in the lower and middle portions of the pluton, and from base to top consists of dunite, clinopyroxene peridotite, olivine gabbro, troctolite, and hornblende gabbro. These rocks exhibit gradual transitions from one layer to another. Olivine in this cycle is mostly serpentinized. Pyroxenes are dominated by

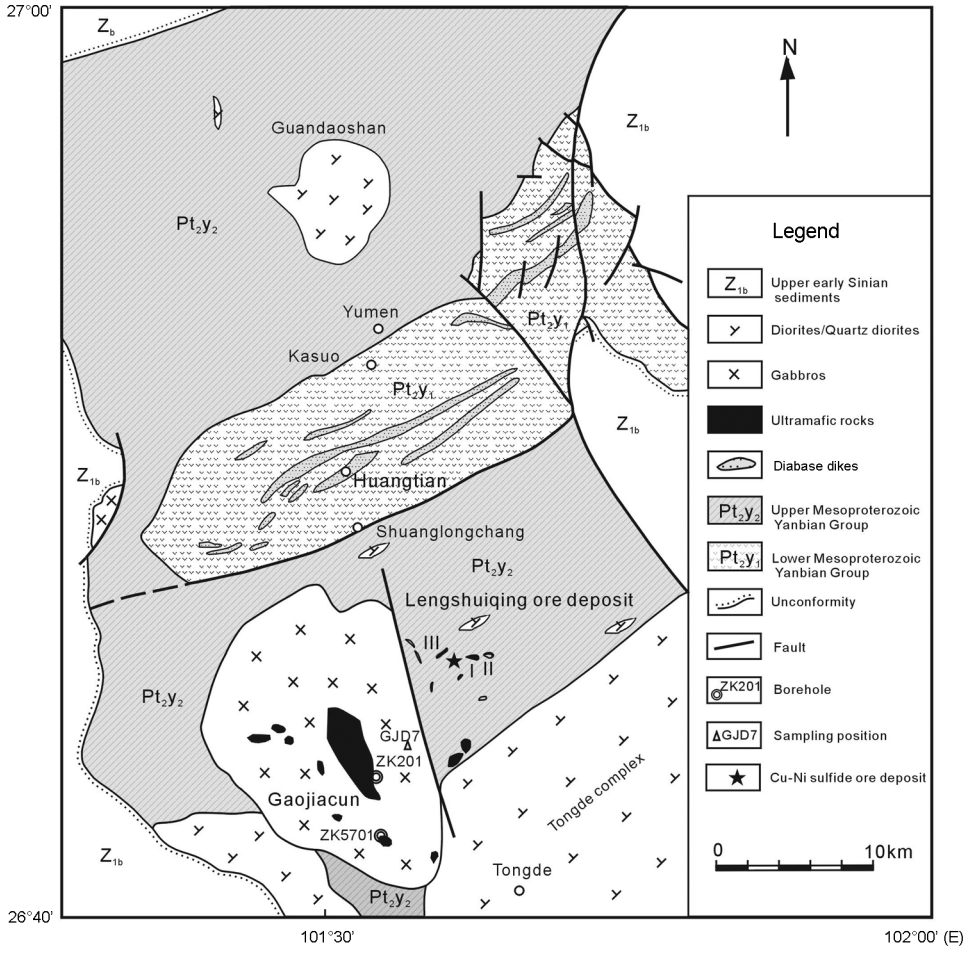

FIG. 2. Simplified Precambrian geological map of the Yanbian area, southwestern Sichuan (modified after Sun, 1994).

clinopyroxene and minor orthopyroxene, with hornblendization observed at the rims of some clinopyroxene crystals. Olivine inclusions occur in clinopyroxene in this cycle. Cycle II in the upper part of the complex consists predominantly of pyroxene hornblende peridotite and hornblende gabbro. Minerals crystallized in the order olivine, clinopyroxene to orthopyroxene, and finally to plagioclase and hornblende. Most of the hornblende is primary. Pyroxene-hornblende peridotite in this cycle is also characterized by olivine inclusions in clinopyroxene. Olivine is quite fresh and orthopyroxene is dominant over clinopyroxene. Cu-Ni sulfide mineralization occurs locally in the pyroxene-hornblende peridotite. Olivines from the Gaojiacun complex, in compositions from $Fo_{71.3}$ to $Fo_{83.6}$, are chrysolite. Clinopyroxenes, in compositions, range mainly from $En_{38.43}$ to $En_{54.02}$, $Fs_{3.11}$ to $En_{34.31}$, and $Wo_{29.65}$ to $Wo_{50.80}$. And orthopyroxenes are from $En_{53.53}$ to $En_{80.87}$, $Fs_{17.47}$ to $Fs_{44.54}$, and $Wo_{0.55}$ to $Wo_{3.47}$ (Zhu, 2004).

Sampling and Analytical Methods

Samples GJD1 and GJD7 used in this study were collected from exposure of the hornblende gabbro in Cycle II of the Gaojiacun complex. Samples GJZ1 to GJZ50 were collected from two representative boreholes (ZK201 and ZK5701) (Fig. 3).

Zircon grains from sample GJD7 were separated using conventional heavy liquid and magnetic techniques. Representative zircon grains were

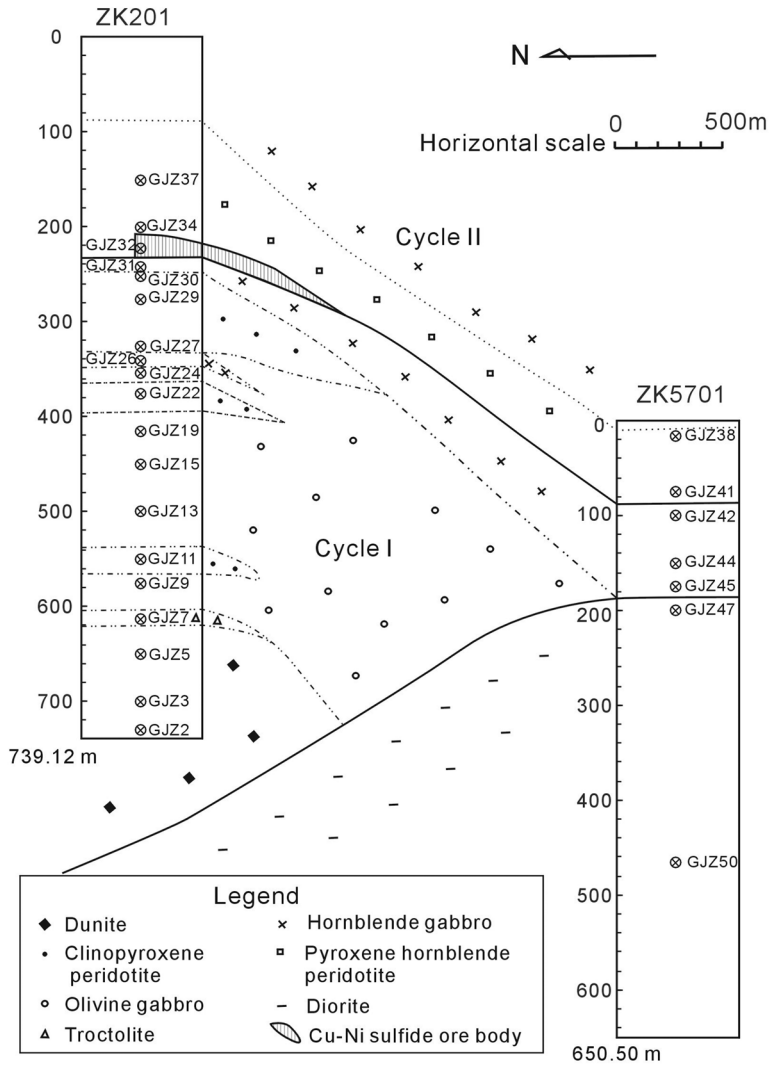

FIG. 3. Cross section from borehole ZK201 to ZK5701 of the Gaojiacun complex and sampling sites.

handpicked using a binocular microscope and mounted in an epoxy resin disc, and then polished and coated with gold film. Zircons were documented with transmitted and reflected light micrographs as well as cathodoluminescence (CL) images to reveal their external and internal structures. The U-Pb isotopic analyses were performed using the Sensitive High-Resolution Ion Microprobe (SHRIMP-II) at the Chinese Academy of Geological Sciences (Beijing). Details of the analytical procedures of zircons using SHRIMP were described by Song et al. (2002) and Jian et al. (2003). Inter-element fractionation ion emission of zircon was corrected relative to the RSES reference TEM (417 Ma). The uncertainties in ages are cited as 1σ, and the weighted mean ages are quoted at the 95% confidence level (2σ).

Major elements were measured by traditional wet chemical analyses at the Center of Analysis and Testing, Institute of Geochemistry, Chinese Academy of Sciences, with an analytical precision better than 1 to 3%. Trace elements were analyzed using ELEMENT ICP-MS at the Key Laboratory of Ore Deposit Geochemistry, Institute of Geochemistry,

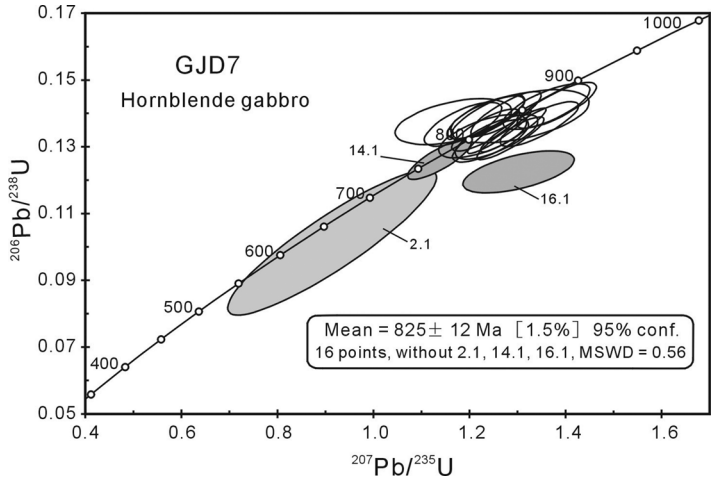

FIG. 4. U-Pb zircon concordia diagram for the Gaojiacun hornblende gabbro (GJD7). The weighted mean $^{206}Pb/^{238}U$ age of 825 ± 12 Ma based on 16 concordant U-Pb analyses (open symbols) is interpreted as the intrusive age of the Gaojiacun complex. The discordant analyses (solid symbols) are due to radiogenic Pb losses.

Chinese Academy of Sciences, using the analytical procedure described by Qi et al. (2000), and the international standards GBPG-1, OU-6, and the French standard UB-N (serpentinite) were used for analytical quality control. The analytical precision is generally better than 5% for trace elements. Sr and Nd isotopic data were obtained in Beijing at the Institute of Geology and Geophysics, Chinese Academy of Sciences, using a multi-collector VG-354 mass spectrometer in static mode. Details of chemical separation and isotopic measurement procedures can be found in Qiao et al. (1987, 1990). The measured $^{87}Sr/^{86}Sr$ and $^{143}Nd/^{144}Nd$ ratios are normalized to $^{86}Sr/^{88}Sr = 0.1194$ and $^{146}Nd/^{144}Nd = 0.7219$, respectively. The $^{87}Sr/^{86}Sr$ ratios of the NBS987 and NBS607 Sr standards and $^{143}Nd/^{144}Nd$ ratios of the BCR-1 and La Jolla Nd standards determined during this study were 0.710240 ± 15 (2σ), 1.20032 ± 30 (2σ), 0.512663 ± 9 (2σ), and 0.511862 ± 7 (2σ), respectively.

Results

Zircon U-Pb data

Zircon grains from sample GJD7 are mostly euhedral, transparent, colorless, and free of inclusions. The CL images display weak euhedral concentric zoning in most crystals, and no inherited zircon was observed. The results of SHRIMP U-Pb analyses on zircons from sample GJD7 are listed in Table 1. Nineteen analyses from this sample were obtained from 19 grains during a single analytical session. Measured U concentrations vary from 40 to 193 ppm, and Th ranges from 24 to 218 ppm. The Th/U ratios range from 0.54 to 1.13. Except for three obviously young $^{206}Pb/^{238}U$ ages of 622 Ma, 745 Ma, and 766 Ma, possibly due to partial loss of radiogenic Pb, the remaining 16 analyses form a single, concordant group with a weighted mean $^{206}Pb/^{238}U$ age of 825 ± 12 Ma (MSWD = 0.56, Fig. 4).

Geochemistry of the Gaojiacun complex

Major- and trace-element data for the Gaojiacun mafic-ultramafic rocks are listed in Table 2. Eight samples were analyzed for Sr-Nd isotopes, and the results are presented in Table 3.

Major-element geochemistry

Rocks from the Gaojiacun mafic-ultramafic complex had been strongly altered, judging by variably high LOI values of 0.5–15.98% (Table 3). The high contents of CaO and CO_2 in some samples from the troctolite and hornblende grabbo units are attributed to carbonatization, as shown by microscopic observations. Thus, major oxides in discussion and schemes below are corrected to a dry magmatic system without volatiles.

In Cycle I, 33.37–35.79%, 32.40–36.90%, 9.96–29.03%, 8.78%, and 9.85–12.51% ranges in MgO contents are for dunite, clinopyroxene peridotite,

TABLE 1. SHRIMP U-Pb Isotopic Data for Zircons from Sample GJD7 in the Gaojiacun Complex[1]

Spot	U, ppm	Th, ppm	Th/U	^{206}Pbc, %	^{206}Pb*, ppm	Isotopic ratio						Age/Ma	
						^{207}Pb*/^{206}Pb*	± %	^{207}Pb*/^{235}U	± %	^{206}Pb*/^{238}U	± %	^{206}Pb/^{238}U	^{207}Pb/^{206}Pb
1.1	83	69	0.83	0.23	10.1	0.0695	3.0	1.360	4.4	0.1420	3.2	856 ± 26	913 ± 62
2.1	86	77	0.90	0.81	7.54	0.0654	6.8	0.910	16	0.1010	14	622 ± 84	788 ± 140
3.1	59	32	0.54	0.36	6.74	0.0684	2.7	1.244	4.2	0.1318	3.2	798 ± 24	882 ± 57
4.1	44	33	0.75	1.23	5.31	0.0615	6.0	1.166	6.9	0.1375	3.3	830 ± 26	657 ± 130
5.1	46	32	0.70	0.26	5.36	0.0713	2.3	1.345	4.0	0.1368	3.2	827 ± 25	967 ± 48
6.1	138	155	1.12	0.10	15.9	0.0680	1.3	1.262	3.5	0.1346	3.2	814 ± 25	869 ± 27
7.1	70	59	0.84	0.72	8.32	0.0629	3.2	1.186	4.5	0.1367	3.2	826 ± 25	705 ± 68
8.1	81	70	0.86	0.00	9.18	0.0703	1.7	1.285	3.6	0.1325	3.2	802 ± 24	938 ± 34
9.1	48	39	0.81	0.63	5.49	0.0669	3.7	1.227	4.9	0.1331	3.2	806 ± 24	834 ± 78
10.1	81	80	0.99	0.34	9.73	0.0647	2.5	1.238	4.1	0.1388	3.2	838 ± 25	764 ± 53
11.1	141	141	1.00	0.00	16.8	0.0645	2.9	1.234	4.3	0.1389	3.1	838 ± 24	757 ± 62
12.1	82	68	0.83	0.12	9.89	0.0662	2.1	1.276	3.8	0.1399	3.1	844 ± 25	812 ± 44
13.1	123	136	1.11	0.00	14.2	0.0694	1.3	1.291	35	0.1350	3.2	816 ± 25	910 ± 27
14.1	58	49	0.84	0.09	6.26	0.0654	2.2	1.138	3.9	0.1263	3.2	766 ± 23	786 ± 46
15.1	128	139	1.09	0.38	14.8	0.0663	2.2	1.233	3.8	0.1350	3.1	816 ± 24	815 ± 46
16.1	40	28	0.70	0.30	4.23	0.0771	4.8	1.302	5.9	0.1225	3.4	745 ± 24	1124 ± 96
17.1	41	30	0.73	0.24	4.70	0.0685	3.1	1.253	4.5	0.1329	3.3	805 ± 25	885 ± 64
18.1	193	218	1.13	0.20	23.6	0.0704	2.3	1.381	4.0	0.1424	3.2	858 ± 26	939 ± 48
19.1	43	24	0.56	0.81	5.19	0.0681	6.2	1.305	7.3	0.1390	3.8	839 ± 30	870 ± 130

[1]Errors are 1-sigma; ^{206}Pbc and Pb* indicate the common and radiogenic portions, respectively. Error in standard calibration was 0.75% (not included in above errors, but required when comparing data from different mounts). Common Pb corrected using measured ^{204}Pb.

TABLE 2. Major- and Trace-Element Data for the Gaojiacun Complex[1]

Sample no.:	GJZ2	GJZ3	GJZ5	GJZ11	GJZ22	GJZ27	GJZ29	GJZ30	GJZ9	GJZ13	GJZ15	GJZ19	GJZ24
Rock type:	DUN	DUN	DUN	CPD	CPD	CPD	CPD	CPD	OGA	OGA	OGA	OGA	OGA
Cycle:	I	I	I	I	I	I	I	I	I	I	I	I	I
							Major element, %						
SiO_2	37.11	35.56	34.96	35.95	35.30	36.49	31.30	36.15	40.68	37.03	35.47	37.76	43.82
TiO_2	0.01	0.01	0.12	0.09	0.21	0.09	0.13	0.01	0.43	0.34	0.09	0.06	0.18
Al_2O_3	5.87	3.65	7.66	0.99	5.60	0.99	7.87	0.85	23.24	8.77	10.16	6.84	12.90
Fe_2O_3	5.12	5.64	4.41	7.89	5.30	6.30	6.24	6.66	1.53	4.93	5.00	5.87	2.48
FeO	6.00	6.05	5.90	6.69	6.85	7.20	7.10	6.35	3.10	4.70	6.10	6.60	4.70
MnO	0.21	0.17	0.15	0.19	0.22	0.15	0.24	0.19	0.08	0.15	0.14	0.25	0.12
MgO	28.79	30.33	28.64	29.38	27.36	29.64	27.96	30.94	9.46	25.47	26.05	25.16	13.96
CaO	2.65	2.63	2.61	1.84	3.07	2.35	1.58	2.36	15.22	6.67	6.01	5.55	13.20
Na_2O	0.43	0.63	0.45	0.27	0.45	0.34	0.03	0.27	1.01	0.60	0.61	0.64	1.04
K_2O	0.07	0.06	0.06	0.17	0.08	0.06	0.02	0.05	0.07	0.17	0.09	0.08	0.08
P_2O_5	0.01	0.01	0.01	0.02	0.01	0.01	0.13	0.01	0.15	0.01	0.02	0.01	0.01
LOI	12.94	14.92	14.37	15.98	15.30	15.90	16.90	15.50	0.50	10.50	10.13	10.66	4.90
CO_2	–	–	–	–	–	–	–	–	4.10	–	–	–	2.10
Total	99.21	99.66	99.34	99.46	99.75	99.52	99.50	99.34	99.57	99.34	99.87	99.48	99.49
$Mg^{\#}$	82.9	82.9	83.8	79.2	80.8	80.4	79.7	81.7	79.0	83.2	81.4	79.1	78.2
							Trace element, ppm						
V	56.8	70.4	63.3	92.3	95.9	91.1	87.0	90.4	65.0	108	88.5	103	115
Cr	3050	3516	3515	3145	3016	3090	3461	3532	521	2350	1209	2976	1205
Ni	928	812	749	961	590	705	639	687	115	493	336	467	228
Cu	87.1	115	55.2	395	57.8	33.7	23.8	38.8	16.2	90.5	73.5	38.7	60.6
Ga	5.15	4.80	4.57	3.76	3.77	4.63	4.11	3.98	12.7	5.33	4.71	5.07	8.04
Rb	0.540	0.652	0.604	0.555	0.500	0.757	0.591	0.581	0.600	0.569	0.446	0.588	0.298
Sr	32.7	12.4	21.9	40.6	48.2	15.1	20.1	16.3	1005	170	200	119	426
Y	0.602	0.634	0.404	0.901	1.44	1.03	0.767	0.908	1.28	2.46	2.25	1.74	3.97
Zr	0.906	1.27	0.702	1.79	3.66	3.37	1.73	2.94	2.93	4.52	4.33	3.11	5.44
Nb	0.029	0.039	0.026	0.023	0.060	0.058	0.017	0.055	0.081	0.048	0.043	0.055	0.060
Cs	0.086	0.033	0.069	0.034	0.035	0.027	0.055	0.026	0.064	0.032	0.083	0.040	0.041
Ba	13.8	5.86	4.19	5.22	6.17	5.57	8.29	7.34	45.2	13.1	15.6	9.83	22.6
La	0.131	0.266	0.172	0.185	0.334	0.442	0.251	0.288	0.611	0.391	0.391	0.437	0.636
Ce	0.329	0.570	0.394	0.490	0.960	1.15	0.647	0.785	1.39	1.23	1.24	1.12	1.76
Pr	0.046	0.080	0.051	0.073	0.136	0.152	0.096	0.114	0.225	0.222	0.210	0.186	0.310
Nd	0.199	0.495	0.244	0.375	0.863	0.812	0.489	0.580	1.11	1.30	1.30	0.896	1.86
Sm	0.054	0.128	0.080	0.161	0.260	0.188	0.168	0.185	0.284	0.400	0.348	0.329	0.629
Eu	0.059	0.080	0.063	0.080	0.126	0.117	0.082	0.075	0.256	0.217	0.210	0.178	0.313
Gd	0.053	.105	0.070	0.153	0.322	0.258	0.175	0.180	0.351	0.467	0.419	0.373	0.666
Tb	0.009	0.019	0.009	0.023	0.040	0.032	0.024	0.029	0.044	0.076	0.080	0.059	0.114
Dy	0.049	0.095	0.055	0.139	0.243	0.196	0.166	0.150	0.334	0.459	0.409	0.305	0.612
Ho	0.012	0.023	0.013	0.030	0.054	0.039	0.031	0.031	0.052	0.097	0.084	0.061	0.111
Er	0.042	0.061	0.042	0.087	0.162	0.100	0.091	0.086	0.149	0.233	0.213	0.166	0.310
Tm	0.005	0.009	0.007	0.009	0.019	0.008	0.009	0.009	0.021	0.030	0.030	0.023	0.038
Yb	0.035	0.049	0.034	0.069	0.134	0.083	0.077	0.080	0.145	0.216	0.167	0.126	0.228
Lu	0.007	0.008	0.006	0.015	0.020	0.011	0.007	0.011	0.017	0.026	0.021	0.020	0.033
Hf	0.032	0.042	0.020	0.067	0.118	0.108	0.062	0.072	0.100	0.206	0.176	0.114	0.211
Ta	0.006	0.009	0.009	0.005	0.007	0.011	0.006	0.013	0.008	0.006	0.009	0.009	0.007
Pb	1.63	2.30	1.41	1.14	1.46	0.659	9.10	1.10	21.0	1.20	1.78	1.56	1.16
Th	0.010	0.010	0.006	0.006	0.036	0.024	0.019	0.020	0.039	0.012	0.019	0.018	0.018
U	0.004	0.004	0.004	0.007	0.015	0.006	0.005	0.012	0.014	0.008	0.011	0.010	0.032

Table continues

TABLE 2. *Continued*

Sample no.:	GJZ7	GJZ26	GJZ31	GJZ45	GJZ44	GJZ42	GJZ32	GJZ41	GJZ34	GJZ37	GJZ38	GJD1	GJD7
Rock type:	TRO	HGA	HGA	HGA	HGA	HGA	PHP (O)	PHP	PHP	PHP	PHP	HGA	HGA
Cycle:	I	I	I	I	I	I	II	II	II	II	II	II	II
							Major element, %						
SiO_2	41.02	43.48	48.76	42.81	40.78	34.63	35.37	37.67	42.33	35.86	36.92	42.05	49.33
TiO_2	0.01	0.80	0.49	0.89	0.86	1.26	0.03	0.40	0.15	0.03	0.27	1.48	1.08
Al_2O_3	26.78	15.45	16.31	19.74	20.67	16.80	5.60	2.43	1.15	7.06	10.23	20.00	21.16
Fe_2O_3	1.10	0.45	3.59	1.91	2.53	6.71	9.12	6.91	5.32	5.75	5.77	3.46	3.94
FeO	2.90	5.09	4.00	6.10	5.90	11.00	5.28	6.24	6.70	6.30	6.10	6.55	4.90
MnO	0.05	0.17	0.20	0.15	0.20	0.19	0.14	0.16	0.20	0.18	0.20	0.21	0.28
MgO	8.21	8.39	7.65	8.61	11.93	7.65	28.84	29.63	26.77	29.98	25.70	8.17	3.90
CaO	11.57	16.72	10.98	11.53	9.06	11.40	1.24	3.39	5.58	1.64	2.36	11.42	9.03
Na_2O	1.75	2.26	3.07	2.96	2.69	2.52	0.72	0.73	0.68	0.40	0.83	2.94	4.13
K_2O	0.14	0.13	1.56	0.60	0.51	0.25	0.16	0.09	0.06	0.10	0.11	0.29	0.21
P_2O_5	0.01	0.26	0.90	0.08	0.22	1.50	0.02	0.01	0.01	0.01	0.01	0.15	0.42
LOI	3.87	0.45	1.40	3.42	4.30	5.09	11.65	11.97	10.80	11.99	10.82	2.10	1.03
CO_2	2.40	5.90	0.30	0.72	–	0.30	1.30 (S)	–	–	–	–	0.63	–
Total	99.81	99.55	99.21	99.52	99.65	99.30	99.47	99.63	99.75	99.30	99.32	99.45	99.41
$Mg^{\#}$	79.0	73.1	65.2	66.2	72.2	44.5	79.2	80.9	80.6	82.3	80.2	60.1	45.1
							Trace element, ppm						
V	6.16	83.8	181	406	183	520	80.6	99.2	117	47.6	97.7	519	245
Cr	26.6	519	470	69.9	452	7.62	3216	2073	1505	1985	2138	135	48.3
Ni	109	148	221	40.3	179	12.4	2164	810	821	887	677	95.5	8.98
Cu	20.7	12.7	110	61.1	47.7	79.4	684	14.7	171	107	13.0	109	36.6
Ga	11.9	12.6	20.9	16.9	15.9	23.1	3.75	6.37	3.61	4.51	6.49	19.0	23.2
Rb	1.03	1.12	5.73	9.00	7.16	1.33	2.03	0.372	0.535	2.24	0.985	1.24	1.04
Sr	968	118	643	842	698	643	23.0	125	41.0	62.8	115	717	909
Y	0.644	17.6	37.8	14.9	12.1	23.4	1.49	2.14	2.93	0.772	2.82	17.2	21.0
Zr	1.56	52.2	45.5	17.9	33.7	24.5	6.14	7.62	10.1	6.79	10.2	26.3	46.5
Nb	0.050	4.80	5.18	1.23	2.19	1.71	0.214	0.393	0.256	0.219	0.429	1.94	9.19
Cs	0.089	0.092	2.64	0.583	0.453	0.219	0.094	0.039	0.048	0.101	0.056	0.066	0.067
Ba	56.6	31.4	659	272	231	150	26.7	32.6	17.9	45.5	43.1	173	386
La	0.413	15.2	34.5	1.65	5.77	9.18	1.83	1.03	1.14	1.43	1.10	3.01	18.5
Ce	0.791	30.1	86.0	6.16	16.8	28.3	3.59	2.77	3.00	2.71	3.06	9.75	43.6
Pr	0.096	3.66	11.2	1.20	2.55	4.67	0.369	0.411	0.480	0.298	0.518	1.84	5.55
Nd	0.450	15.7	48.5	7.25	13.6	25.4	1.39	1.86	2.48	1.18	2.62	9.75	26.7
Sm	0.077	3.57	11.3	2.48	3.18	6.32	0.291	0.451	0.635	0.206	0.607	3.67	5.65
Eu	0.185	0.847	2.58	1.14	1.25	2.51	0.096	0.219	0.289	0.085	0.299	1.57	2.70
Gd	0.055	3.50	9.69	2.85	2.79	6.22	0.242	0.458	0.787	0.177	0.691	3.98	5.61
Tb	0.009	0.551	1.47	0.474	0.404	0.983	0.042	0.065	0.109	0.022	0.100	0.630	0.820
Dy	0.035	2.82	7.52	2.80	2.56	4.84	0.206	0.372	0.631	0.143	0.520	3.64	4.12
Ho	0.010	0.629	1.46	0.564	0.453	0.973	0.051	0.076	0.115	0.020	0.112	0.732	0.798
Er	0.025	1.58	3.56	1.35	1.17	2.24	0.098	0.218	0.288	0.075	0.271	1.64	1.91
Tm	0.004	0.247	0.465	0.169	0.161	0.267	0.016	0.023	0.043	0.008	0.039	0.213	0.287
Yb	0.021	1.45	2.93	1.13	1.01	1.71	0.122	0.199	0.255	0.079	0.223	1.33	1.68
Lu	0.004	0.232	0.418	0.172	0.156	0.226	0.018	0.031	0.032	0.011	0.036	0.184	0.246
Hf	0.031	1.52	2.03	1.01	1.22	1.13	0.199	0.197	0.295	0.183	0.320	1.09	3.13
Ta	0.005	0.266	0.355	0.101	0.072	0.065	0.014	0.024	0.018	0.019	0.026	0.087	0.446
Pb	1.57	4.20	11.1	1.20	4.23	3.80	6.29	0.285	0.535	0.720	0.496	2.57	4.03
Th	0.013	2.53	3.24	0.024	0.054	0.092	0.175	0.041	0.104	0.186	0.084	0.087	0.224
U	0.012	0.807	3.05	0.031	0.024	0.047	0.086	0.027	0.024	0.078	0.026	0.032	0.098

[1]$Mg^{\#}$ = 100*molar MgO/(Mg+FeO) with FeO as total Fe; LOI = loss on ignition; DUN = dunite; CPD = clinopyroxene peridotite; OGA = olivine gabbro; TRO = troctolite; HGA = hornblende gabbro; PHP = pyroxene hornblende peridotite; PHP (O) = pyroxene hornblende peridotite bearing Cu-Ni sulfide ore; "–" = not determined.

TABLE 3. Sr and Nd Isotopic Results for the Gaojiacun Complex[1]

Sample no.:	GJZ-15	GJZ-24	GJZ-7	GJZ-32	GJZ-41	GJZ-38	GJD-1	GJD-7
Rock type:	OGA	OGA	TRO	PHP (O)	PHP	PHP	HGA	HGA
Rb (ppm)	0.446	0.298	1.03	2.03	0.372	0.985	1.24	1.04
Sr (ppm)	200	426	968	23	125	155	717	909
$^{87}Rb/^{86}Sr$	0.0065	0.0020	0.0031	0.2550	0.0086	0.0247	0.0050	0.0033
$^{87}Sr/^{86}Sr$	0.705057	0.704814	0.704925	0.707606	0.704713	0.704882	0.704730	0.704621
(2σ)	(19)	(20)	(18)	(20)	(18)	(17)	(19)	(16)
$(^{87}Sr/^{86}Sr)_i$	0.704980	0.704900	0.704888	0.704601	0.704612	0.704591	0.704671	0.704582
Sm (ppm)	0.347	0.629	0.077	0.291	0.451	0.607	3.00	5.71
Nd (ppm)	1.30	1.86	0.450	1.39	1.86	2.62	9.17	25.6
$^{147}Sm/^{144}Nd$	0.1621	0.2040	0.1039	0.1268	0.1466	0.1401	0.1981	0.1348
$^{143}Nd/^{144}Nd$	0.512661	0.512727	0.512200	0.512355	0.512439	0.512449	0.512720	0.512394
(2σ)	(11)	(10)	(11)	(6)	(8)	(10)	(9)	(7)
$(^{143}Nd/^{144}Nd)_i$	0.511784	0.511623	0.511638	0.511669	0.511646	0.511691	0.511648	0.511665
$\varepsilon_{Nd}(i)$	+4.5	+1.3	+1.6	+2.2	+1.8	+2.7	+1.8	+2.2

[1]Chondrite uniform reservoir (CHUR) values ($^{87}Rb/^{86}Sr = 0.0847$, $^{87}Sr/^{86}Sr = 0.7045$; $^{147}Sm/^{144}Nd = 0.1967$, $^{143}Nd/^{144}Nd = 0.512638$) are used for the calculation. $M_{Rb} = 1.42 \times 10^{-11}year^{-1}$ (Steiger and Jäger, 1977); $M_{Sm} = 6.54 \times 10^{-12}year^{-1}$ (Lugmair and Harti, 1978). The $(^{87}Sr/^{86}Sr)_i$, $(^{143}Nd/^{144}Nd)_i$, and $\varepsilon_{Nd}(i)$ of the Gaojiacun complex were calculated at the age of 825 Ma.

olivine gabbro, troctolite, and hornblende gabbro units, respectively. Mg# decreases from 82.9–83.8 for the dunite unit, 79.2–81.7 for the clinopyroxene peridotite unit, 79.0–83.2 for the olivine gabbro unit, 79.0 for the troctolite unit, and to 44.5–73.1 for hornblende grabbo unit. In Cycle II, 29.04–34.34% and 3.96–8.45% ranges in MgO contents are for the pyroxene-hornblende peridotite unit and the hornblende gabbro unit, respectively. Mg# decreases from 80.2–82.3 in the pyroxene-hornblende peridotite unit to 44.5–60.1 in the hornblende gabbro unit. SiO_2, TiO_2, and Al_2O_3 contents increase with decreasing MgO contents, whereas corresponding FeO* contents decrease in Cycles I and II (Fig. 5).

Trace-element geochemistry

The ultramafic rocks in this complex are characterized by low incompatible-element and high compatible-element (Cr, Ni) contents (Table 2; Fig. 5). The compatible elements reflect mineral compositions, whereas the incompatible elements reflect the trapped liquid component in the rocks.

In Cycle I, REE contents are 1.03–1.99, 1.89–3.67, 2.88–7.62, and 51.8–221 ppm for dunite, clinopyroxene peridotite, olivine gabbro, and hornblende gabbro units, respectively. In chondrite-normalized REE patterns (Fig. 6A), most of the samples in this cycle are slightly to moderately enriched in LREE, with variable positive Eu anomalies ($(La/Yb)_N = 0.98–7.95$, $\delta Eu = 0.73–8.69$). In contrast, the troctolite unit is characterized by low REE abundance, remarkable REE fractionation, and a positive Eu anomaly ($\Sigma REE = 2.18$ ppm, $(La/Yb)_N = 13.26$, $\delta Eu = 8.69$). REE contents in Cycle II are obviously higher than those in Cycle I—that is, 6.44–10.2 ppm for the pyroxene-hornblende peridotite unit and 41.9–118 ppm for the hornblende gabbro unit. The pyroxene-hornblende peridotite unit displays moderate to high LREE enrichment and a slightly positive Eu anomaly ($(La/Yb)_N = 3.01–12.20$, $\delta Eu = 1.11–1.47$). The hornblende gabbro unit shows moderate LREE enrichment with a slightly positive Eu anomaly ($(La/Yb)_N = 1.53–7.40$, $\delta Eu = 1.26–1.46$) (Fig. 6C). The shape of the REE patterns for Cycle II are also quite different from cycle I, except for the hornblende gabbro, which is similar for both cycles.

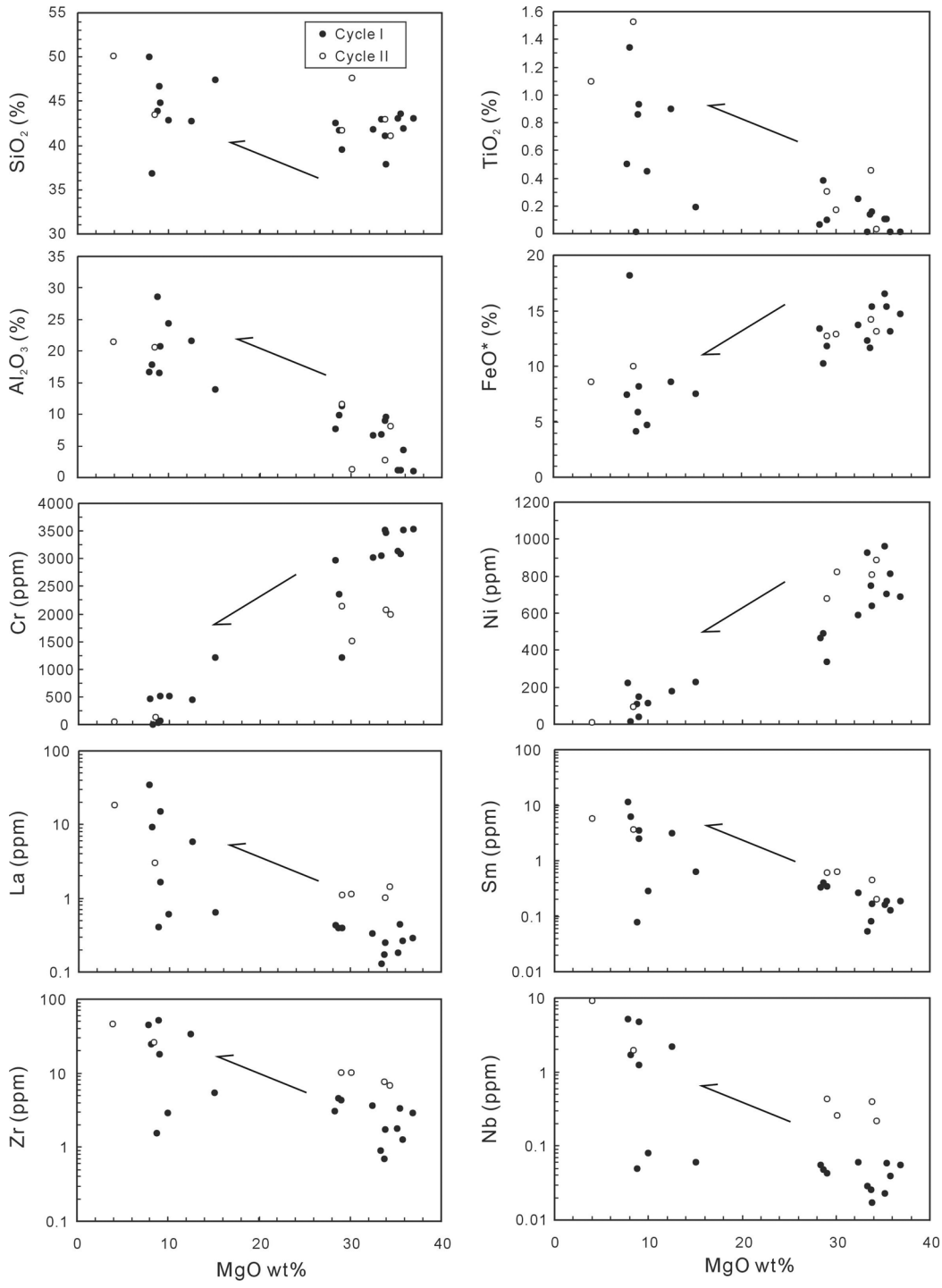

FIG. 5. Plots of major oxides (SiO_2, TiO_2, Al_2O_3, and FeO*) (recalculated 100 wt% oxides free of volatiles) and trace-element contents (Cr, Ni, La, Sm, Zr, and Nb) versus MgO wt%, illustrating the main trends exhibited by rock samples of the Gaojiacun complex.

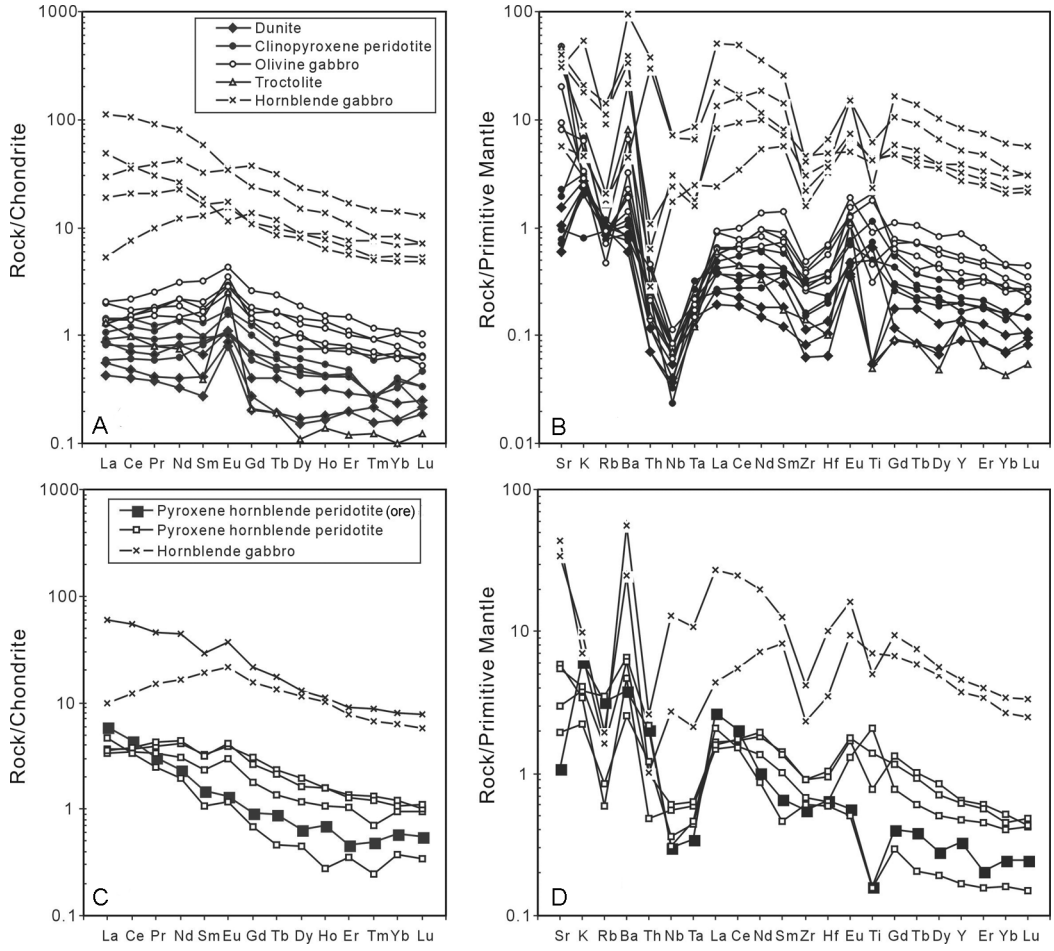

FIG. 6. Chondrite-normalized REE diagrams (A, C) and primitive mantle–normalized incompatible-element distribution spridergrams (B, D) for the Gaojiacun complex (A and B for Cycle I, C and D for Cycle II). The normalization values of chrondrite and primitive mantle are from Boynton (1984) and Sun and McDonough (1989), respectively.

In the primitive mantle–normalized trace-element "spider diagram" (Figs. 6B and 6D), most of the samples from the complex are depleted in high-field-strength elements (Th, Nb, Ta, Zr, and Hf) and relatively enriched in large ion lithophile elements (Ba and Sr).

Sr-Nd isotopes

The rock units of the Gaojiacun complex have small ranges of $^{87}Sr/^{86}Sr$ (0.7046–0.7051) and low values of $^{87}Rb/^{86}Sr$ (0.0020-0.0255), whereas the ore-bearing units have higher $^{87}Sr/^{86}Sr$ (0.7076) and $^{87}Rb/^{86}Sr$ ratios (0.2550). All the samples have small ranges of $(^{87}Sr/^{86}Sr)_i$ (0.7045–0.7050) (Fig. 7). These samples have $^{147}Sm/^{144}Nd$ and $^{143}Nd/^{144}Nd$ ratios varying from 0.1039 to 0.2040 and from 0.512200 to 0.512727, respectively, with $\varepsilon_{Nd}(i)$ values of +1.3 to +4.5 (Fig. 7). The samples display low $(^{87}Sr/^{86}Sr)_i$ and positive $\varepsilon_{Nd}(i)$ ratios, indicative of magmas derived from a depleted mantle source.

Discussion

Emplacement age of the complex

SHRIMP zircon U-Pb dating indicates that the hornblende gabbro in Cycle II of the Gaojiacun complex was formed at 825 ± 12 Ma. This is consistent with the SHRIMP zircon U-Pb ages of the

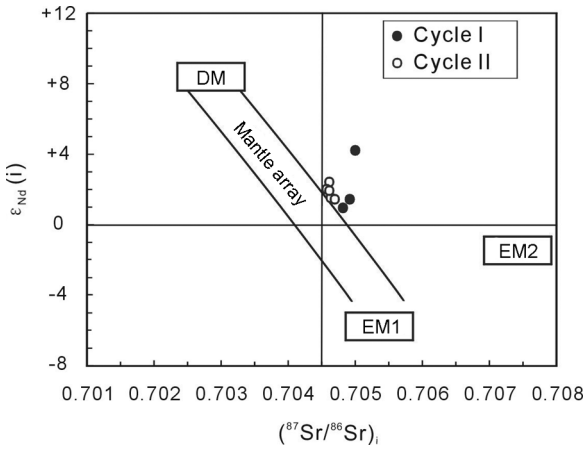

FIG. 7. Plot of initial $\varepsilon_{Nd}(i)$ and $(^{87}Sr/^{86}Sr)_i$ (t = 825 Ma) for the Gaojiacun complex. The approximate fields for DM, EM1, and EM2 are from Zindler and Hart (1986).

Tongde gabbro-diorite (820 ± 13 Ma) and diorite (813 ± 14 Ma) along the southeastern and southwestern margins of the Gaojiacun complex (Sinclair, 2001).

Previous studies suggested that Neoproterozoic felsic magmatic rocks are widespread, whereas coeval mafic magmatic rocks are volumetrically minor (Li X. H. et al., 2002b). However, geochronological study of the Gaojiacun complex confirms that intense Neoproterozoic mafic magmatism also occurred on the western margin of the Yangtze craton. Comparatively, SHRIMP U-Pb zircon dating of the large Wangjiangshan and Bijigou complexes on the northwestern margin of the Yangtze craton has yielded ages of 808–819 Ma and 782 Ma, respectively (Zhou M. F. et al., 2002a). All the above studies suggest that intensive mafic magmatism occurred during the Neoproterozoic along the western and northwestern margins of the Yangtze craton.

Magmatic evolution

Petrographically, rocks of the layered intrusions appear to be crystal cumulates, and this is confirmed by the geochemical data. Chilled margins have not been observed in the Gaojiacun complex, and no closely related mafic dikes have been identified as possible feeders; hence there is no direct evidence of the composition of the parent magmas, which makes estimation of the primary magma composition difficult.

SiO_2-Al_2O_3 plots for clinopyroxene compositions of Le Bas (1962) are useful in the classification of slowly cooled, coarse-grained igneous rocks (Coish and Taylor, 1979). The clinopyroxenes plot in the subalkaline field of Le Bas (1962) (Fig. 8A). In addition, most of the clinopyroxenes occupy the calc-alkali basalt field on the Ti-Alt discrimination diagram of Leterrier et al. (1982) (Fig. 8B). It is therefore likely that the parental magma in equilibrium with the clinopyroxene compositions of the Gaojiacun complex was subalkaline basaltic in chemistry.

Compatible-element (Cr, Ni) contents of the Gaojiacun complex gradually decrease with decreasing MgO contents and Mg# values, whereas incompatible element contents gradually increase upwards in the two cumulative cycles. This trend is consistent with fractional crystallization. However, simple fractional crystallization cannot explain the abrupt changes of Mg#, Cr, Ni, and incompatible elements contents across the boundary of the two cycles. Thus, the two cumulative cycles of the Gaojiacun complex were probably produced by two pulses of parental magma and crystal fractionation.

Crustal contamination

Continental crust is typically low in TiO_2 content and highly depleted in Ta and Nb (Rudnick and Fountain, 1995; Barth et al, 2000). Most of the samples from the Gaojiacun complex are depleted in Nb, Ta, and enriched in Ba and Sr. Furthermore, initial Nd-Sr isotope ratios of the intrusive complex lie to the right of the mantle array in the $\varepsilon_{Nd}(i)$–$(^{87}Sr/^{86}Sr)_i$ diagram (Fig. 7). These elemental and isotopic

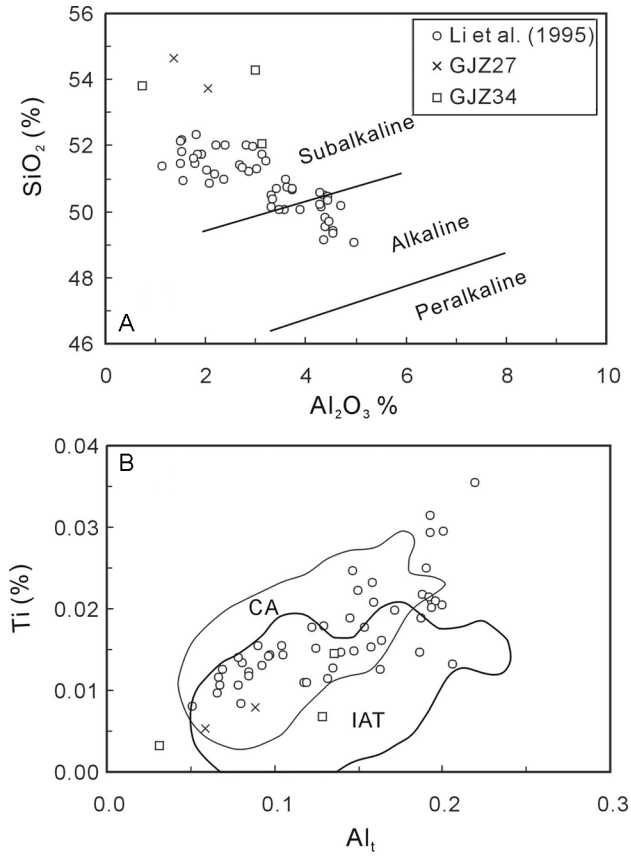

FIG. 8. SiO_2-Al_2O_3 diagram (A) of Le Bas (1962) and Ti-Al_t discrimination plots (B) of Leterrier et al. (1982) for clinopyroxene of the Gaojiacun complex (data from Li H., 1995; Zhu W. Z., 2004). Abbreviations: CA = calc-alkaline; IAT = island-arc tholeiite.

characteristics indicate that the parental magma of the Gaojiacun complex was contaminated by crustal materials.

In some cases, magma contamination and source enrichment can both contribute to enriched isotopic and trace-element signatures (Huppert and Sparks, 1985; Lambert et al., 1989; Lambert et al., 1994). Obvious covariations between ε_{Nd} and 1/Nd, except for GJZ7 with low Nd content, are observed in the $\varepsilon_{Nd}(i)$–1/Nd diagram (Fig. 9A) (Faure, 1986), suggesting that the magma parental of the Gaojiacun complex was intensively contaminated by crustal materials. Contamination could therefore have occurred during the ascent stage, rather than in the magma chamber or primary melting stage. This contamination resulted in the observed depletion of Nb and Ta.

Upper continental crust is enriched in Th, whereas lower continental crust is not usually enriched in this element (Rudnick and Fountain, 1995). Gaojiacun rock samples have quite low Th contents. Furthermore, most of the samples define a line that could represent mixing between mantle melts and lower continental crust in the $(Th/Ta)_{PM}$ vs. $(La/Ta)_{PM}$ diagram (Fig. 9B) (Ingle et al., 2002). These variations are consistent with contamination derived from the lower crust rather than from the upper crust.

As a result, crustal contamination and fractional crystallization were critical for the formation of the Gaojiacun intrusive complex, similar to the process of magmatic assimilation and fractional crystallization (AFC). The combination of crustal contamination and fractionation may have important

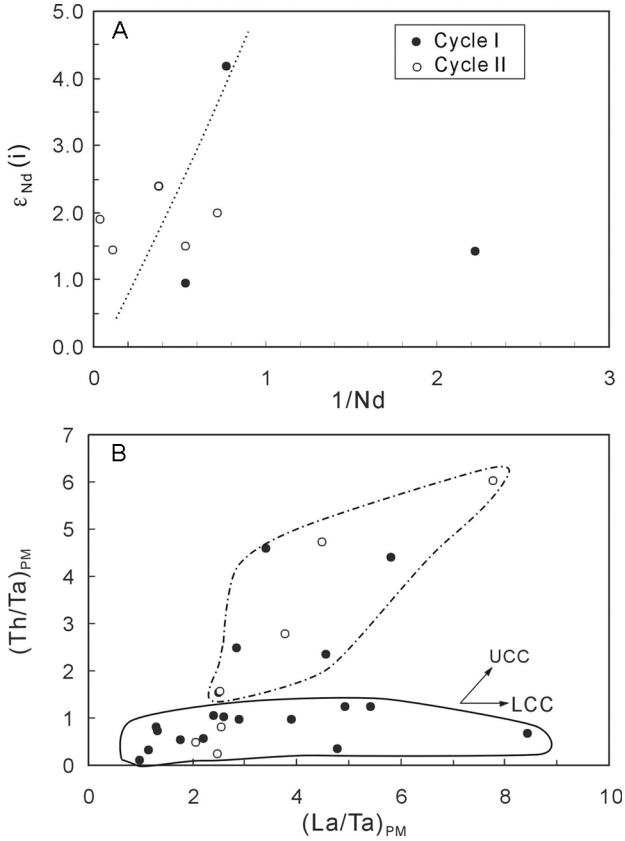

FIG. 9. Variations of $\varepsilon_{Nd}(i)$ vs.1/Nd diagram (A) (Faure, 1986) and (Th/Ta)PM vs. (La/Ta)PM diagram (B) (Ingle et al., 2002) for the the Gaojiacun complex. Abbreviations: UCC = upper crust; LCC = lower crust.

implications for the formation of sulfide zones within layered intrusions (Naldrett, 2004).

Tectonic significance

Previous studies suggested that the Gaojiacun complex was a portion of the Proterozoic "Yanbian Ophiolite" (Geological Team, 1975). However, the present study and recent research argue against the existence of the "Yanbian Ophiolite" on the basis of the following evidence: (1) The Gaojiacun complex intruded metavolcanic rocks and schists of the Mesoproterozoic Yanbian Group. (2) There is no evidence for a dike complex at the boundary between the Gaojiacun pluton and the metavolcanic rocks of the Yanbian Group in the studied region. Olivine inclusions occur in clinopyroxene from the complex, indicating that metamorphic peridotite did not exist in the Gaojiacun complex. Furthermore, the diabase dike swarms, 10 km north of the complex, show an obvious intrusive relationship with pillow basalts of the Yanbian Group. (3) The hornblende gabbro in the main rock phase of the complex was emplaced at 825±12 Ma, showing that there is no genetic relationship between the pluton and the metavolcanic rocks of the Mesoproterozoic Yanbian Group. In addition, the Yanbian volcanic rocks are enriched in LREE, which are significantly different from LREE-depleted N-MORB within ophiolites (Sinclair, 2001). (4) Cu-Ni sulfide mineralization is present in the Gaojiacun complex, but this type of deposit rarely occurs in ophiolite complexes.

The mafic-ultramafic dikes and sills in northern Guangxi, the widespread granites of similar ages (819–824 Ma), and rapid uplifting and unroofing in South China, indicate that a mantle plume could have existed underneath South China at ~825 Ma, and this mantle plume initiated Neoproterozoic

continental rifting and magmatism in South China (Li Z. X. et al., 1999). This proposal is also supported by the occurrence of alkaline basalts at Suxiong (Li X. H. et al., 2002a) and Hannan (Ling et al., 2003), which display geochemical and Nd isotopic characteristics very similar to those of typical alkaline basalts in modern oceanic island basalts (OIB) and continental flood basalts (CFB) provinces. As an alternative view, Zhou M. F. et al. (2002a, 2002b; Zhou J. C. et al., 2004) suggested that the eastern, western to northern margin of the Yangtze craton was an active magmatic arc at 865–760 Ma, based on the arc-like geochemical signatures for the granitoid and mafic-ultramafic intrusions.

This study shows for the first time that intensive ~825 Ma mafic magmatism was present on the western margin of the Yangtze craton. The coeval granitoids and mafic-ultramafic intrusions in the Yanbian area correspond constitute bimodal compositions, consistent with modern continental rift phenomena. The Gaojiacun samples have fairly low Th contents, significantly different from tholeiitic basalts in island arcs. Most importantly, the Gaojiacun and Bijigou intrusions were mineralized in V-Ti (Su et al., 1992; Li H. et al., 1995), similar to that of the well-known Pan-Xi giant V-Ti deposits related to the mafic-ultramafic intrusions of the Late Permian Emeishan plume in Southwest China (Zhong et al., 2003, 2004). The Gaojiacun complex is also characterized by Cu-Ni sulfide mineralization in Cycle II, similar to the coeval Lengshuiqing magmatic Cu-Ni sulfide ore deposit to the northeast of the Gaojiacun complex (Zhu et al., 2004b). The majority of world-class magmatic Ni-Cu sulfide deposits are generally related to mantle plume–derived flood basalts (i.e., Noril'sk-Talnakh and Duluth), komatiites (i.e., Kambalda and Thompson), and large layered mafic-ultramafic complexes related to extensional environments (i.e., Bushveld and Great Dyke) (Naldrett, 1997). Thus, the Gaojiacun complex could have formed in an extensional continental rift rather than an island-arc environment. It was most likely related to a mantle superplume underneath the supercontinent Rodinia within an intraplate tectonic setting. The intrusion was generated by cumulation of basaltic magma subjected to crustal contamination.

Conclusions

The following conclusions are drawn on the basis of the new analytical data presented here.

1. SHRIMP zircon U-Pb data indicate that the Gaojiacun layered mafic-ultramafic complex formed at 825 ± 12 Ma. Thus, we believe that intense Neoproterozoic mafic magmatism occurred along the western margin of the Yangtze craton.

2. Samples from the Gaojiacun complex are characterized by low $(^{87}Sr/^{86}Sr)_i$ and positive $\varepsilon_{Nd}(t)$ values, corresponding to a depleted mantle source. The parental magma of the complex is a subalkaline basalt. Crustal contamination and fractional crystallization were critical factors for the formation of the Gaojiacun intrusive complex, similar to the process of magmatic assimilation and fractional crystallization (AFC). The combination of crustal contamination and fractionation may have important implications for the formation of sulfide zones.

3. An argument has been proposed against the concept of the "Yanbian Ophiolite." We suggest that the Gaojiacun complex was formed in a continental rift possibly related to mantle superplume activity beneath Rodinia.

Acknowledgments

We appreciate the assistance of S.-R. Li and Y.-P. Wang for analyses of major and trace elements, Y.-S. Wan for SHRIMP zircon U-Pb dating, and Z.-Y. Chu for analyses of Sr and Nd isotopes. The paper has benefited from the constructive comments of G.-Z. Tu, X.-H. Li, X.-C. Zhang, and Y.-P. Liu. This work was supported jointly by the "CAS Hundred Talents" Foundation of the Chinese Academy of Sciences and a grant from the Knowledge-Innovation Program of the Chinese Academy of Sciences (Grants KZCX2-101 and KZCX3-SW-125).

REFERENCES

Barth, M. G., McDonough, W. F., and Rudnick, R. L., 2000, Tracking the budget of Nb and Ta in the continental crust: Chemical Geology, v. 165, p. 197–213.

Boynton, W. V., 1984, Geochemistry of the rare earth elements: Meteorite studies, *in* Henderson, P., ed., Rare earth element geochemistry: Amsterdam, The Netherlands, Elservier, p. 63–114.

Chen, J. F., Foland, K. A., Xing, F. M., Xu, X., and Zhou, T. X., 1991. Magmatism along the southeastern margin of the Yangtze block: Precambrian collision of the Yangtze and Cathaysia blocks of China: Geology, v. 19, p. 815–818.

Coish, R. A., and Taylor, L. A., 1979, The effect of cooling rate on texture and pyroxene chemistry in DSDP leg 34

basalt: A microprobe study: Earth and Planetary Science Letters, v. 42, p. 389–398.

Cong, B. L., 1988, Formation and evolution of Panxi paleo-rift: Beijing, China, Science Press, 424 p. (in Chinese).

Faure, G., 1986, Principles of isotope geology, 2nd ed.: New York, NY, John Wiley and Sons, 589 p.

Gan, X. C., Li, X. H., Zhao, F. Q., and Huang, H. B., 1996, Zircon U-Pb and Sm-Nd isochron ages of spilite from Danzhou group, Guangxi Zhuang Autonomous region: Geochimica, v. 25, p. 270–276 (in Chinese).

Geological Team 106 of Sichuan Bureau of Geology and Mineral Resource (SBGMR), 1975, Pre-Sinian geologic features of middle section of Kangdian axis and its relationship to relate tectonics: Scientia Geologica Sinica, v. 2, p. 107–113 (in Chinese).

Huppert, H. E., and Sparks, R. S. J., 1985, Cooling and contamination of mafic and ultramafic magmas during ascent through continental crust: Earth and Planetary Science Letters, v. 74, p. 371–386.

Ingle, S., Weis, D., Scoates, J. S., and Frey, F. A., 2002, Relationship between the early Kerguelen plume and continental flood basalts of the paleo-eastern Gondwanan margins: Earth and Planetary Science Letters, v. 197, p. 35–50.

Jian, P., Liu, D. Y., and Sun, X. M., 2003, SHRIMP dating of Carboniferous Jinshajiang ophiolite in western Yuannan and Sichuan: Geochronological constraints on the evolution of the Paleo-Tethys oceanic crust: Acta Geologica Sinica, v. 77, p. 217–277 (in Chinese).

Lambert, D. D., Morgan, J. W., Walker, R. J., Shirey, S. B., Carlson, R. W., Zientek, M. L., and Koski, M. S., 1989, Rhenium-osmium and samarium-neodymium isotopic systematics of the Stillwater Complex: Science, v. 224, p. 1169–1174.

Lambert, D. D., Walker, R. J., Morgan, J. W., Shirey, S. B., Carlson, R. W., Zientek, M. L., Lipin, B. R., Koski, M. S., and Cooper, R. L., 1994. Re-Os and Sm-Nd isotope geochemistry of the Stillwater Complex, Montana: Implications for the petrogenesis of the J-M Reef: Journal of Petrology, v. 35, p. 1717–1753.

Le Bas, M. J., 1962, The role of aluminium in igneous clinopyroxenes with relation to their parentage: American Journal of Science, v. 260, p. 267–288.

Leterrier, J., Maury, R. C., Thonon, P., Girard, D., and Marchal, M., 1982, Clinopyroxene composition as a method of identification of the magmatic affinities of paleo-volcanic series: Earth and Planetary Science Letters, v. 59, p. 139–154.

Li, H., Bai, J. W., Chen, F. L., Zou, X. H., Zheng, X. H., Yang, Z. T., Yang, X., and Hu, X.. F., 1995, Precambrian mafic layered complexes in the northern and western margins of the Yangtze block and their platinum group element characteristics. Xian, China: Northwest University, 128 p. (in Chinese).

Li, J. L., Zhang, F. Q., and Wang, S. X., 1983, Rare-earth element distribution pattern of Proterozoic ophiolite, Yanbian, Sichuan: Petrological Research, v. 3, p. 37–44 (in Chinese).

Li, W. X., Li, X. H., and Li. Z. X., 2005, Neoproterozoic bimodal magmatism in the Cathaysia Block of South China and its tectonic significance: Precambrian Research, v. 136, p. 51–66.

Li, X. H., Li, Z. X., Ge, W., Zhou, H. W., Li, W. X., Liu, Y., and Wingate, M. T. T., 2003, Neoproterozoic granitoids in South China: Crustal melting above a mantle plume at ca. 825 Ma?: Precambrian Research, v. 122, p. 45–83.

Li, X. H., Li, Z. X., Zhou, H., Liu, Y., and Kinny, P. D., 2002a, U-Pb zircon geochronology, geochemistry and Nd isotopic study of Neoproterozoic bimodal volcanic rocks in the Kangding Rift of South China: Implications for the initial rifting of Rodinia: Precambrian Research, v. 113, p. 135–155.

Li, X. H., Li, Z. X., Zhou, H., Liu, Y., and Liang, X. H., 2002b, U-Pb zircon geochronological, geochemical and Nd isotopic study of Neoproterozoic basaltic magmatism in western Sichuan: Petrogensis and geodynamic implications: Earth Science Frontiers, v. 9, p. 329–338 (in Chinese).

Li, X. H., Zhou, G. Q., Zhao, J. X., Fanning, C. M., and Compston, W., 1994, SHRIMP ion microprobe zircon age and Sm-Nd isotopic characteristics of the NE Jiangxi Ophiolite and its tectonic implications: Chinese Journal of Geochemistry, v. 13, p. 317–325.

Li, Z. X., Li, X. H., Kinny, P. D., and Wang, J., 1999, The breakup of Rodinia: Did it start with a mantle plume beneath South China?: Earth and Planetary Science Letters, v. 173, p. 171–181.

Li, Z. X., Li, X. H., Kinny, P. D., Wang, J., Zhang, S., and Zhou, H., 2003, Geochronology of Neoproterozoic syn-rift magmatism in the Yangtze Craton, South China and correlations with other continents: Evidence for a mantle superplume that broke up Rodinia: Precambrian Research, v. 122, p. 85–109.

Li, Z. X., Zhang, L., and Powell, C. M., 1995, South China in Rodinia: Part of the missing link between Australia–east Antarctica and Laurentia? Geology, v. 23, p. 407–410.

Li, Z. X., Zhang, L., and Powell, C. M., 1996, Positions of the East Asian cratons in the Neoproterozoic supercontinent Rodinia: Australian Journal of Earth Sciences, v. 43, p. 593–604.

Ling, W., Gao, S., Zhang, B., Li, H., Liu, Y., and Cheng, J., 2003, Neoproterozoic tectonic evolution of the northwestern Yangtze craton, South China: Implications for amalgamation and break-up of the Rodinia supercontinent: Precambrian Research, v. 122, p. 111–140.

Lugmair, G. W., and Harti, K., 1978. Lunar initial $^{143}Nd/^{144}Nd$: Differential evolution of the lunar crust and mantle: Earth and Planetary Science Letters, v. 39, p. 349–357.

Luo, Y. N., 1983, Paleo-plate history of the Kangdian tectonic belt: Earth Science, v. 3, p. 93–102 (in Chinese).

Naldrett, A. J., 1997, Key factors in the genesis of Noril'sk, Subdury, Jinchuan, Voisey's Bay and other world-class Ni-Cu-PGE deposits: Implications for exploration: Australian Journal of Earth Science, v. 44, p. 283–316.

Naldrett, A. J., 2004, Magmatic sulfide deposits: Geology, geochemistry, and exploration: Heidelberg/Berlin, Germany, Springer Verlag, 728 p.

Qi, L., Hu, J., and Gregoire, D. C., 2000, Determination of trace elements in granites by inductively coupled plasma mass spectrometry; Talanta, v. 51, p. 507–513.

Qiao, G. S., Wang, K. Y., Guo, Q. F., and Zhang, G. C., 1987, Sm-Nd dating of Gaozhang early Archean supercrustals, Eastern Hebei: Scientia Geologica Sinica, v. 22, p. 86–92 (in Chinese).

Qiao, G. S., Zhai, M. G., and Yan, Y. H., 1990, Geochronological study of Archean rocks in Anshan, Liaoning Province: Scientia Geologica Sinica, v. 25, p. 158–165 (in Chinese).

Rudnick, R. L., and Fountain, D. M., 1995, Nature and composition of the continental crust: A lower crustal perspective: Reviews of Geophysics, v. 33, p. 267–309.

SBGMR (Sichuan Bureau of Geology and Mineral Resources), 1991, Regional geology of Sichuan Province: Beijing, China, Geological Publishing House, 680 p. (in Chinese).

Shen, S. Y., Zhang, B., M., and Yuan, Y. M., 1986, Petrological study of the basic-ultrabasic complex in Yanbian, Sichuan Province: Earth Science, v. 11, p. 561–569 (in Chinese).

Shen, W. Z., Gao, J. F., Xu, S. J., Tan, G. Q., Yang, Z. S., and Yang, Q. W., 2003, Age and geochemical characteristics of the Lengshuiqing body, Yanbian, Sichuan Province: Acta Petrologica Sinica, v. 19, p. 27–37 (in Chinese).

Shen, W. Z., Gao, J. F., Xu, S., J., and Zhou, G. Q., 2002, Geochemical characteristics and genesis of the Qiaotou basic complex, Luding County, western Yangtze Block. Geological Journal of China Universities, v. 8, p. 380–389 (in Chinese).

Sinclair, J. A., 2001, A re-examination of the "Yanbian Ophiolite Suite": Evidence for western extension of the Mesoproterozoic Sibao Orogen in South China [abs.]: Geological Society of Australia, v. 65, p. 99–100.

Song, B., Zhang, Y. H., Wan, Y. S., and Jian, P., 2002, Mount making and SHRIMP dating procedure: Geology Review, v. 48 (suppl.), p. 26–30 (in Chinese).

Steiger, R. H., and Jäger, E., 1977, Subcommission on geochronology: Convention on the use of decay constants in geo- and cosmochronology: Earth and Planetary Science Letters, v. 36, p. 359–362.

Su, L., Yang, H. Q., Song, S. G., and Dong, S. Y., 1992, Petrography and mineralization of the Bijigou mafic complex: Northwest Metallurgy Geology Information, v. 4, p. 25–34 (in Chinese).

Sun, C. M., 1994, Genetic mineralogy of pyroxenes from the Yanbian Proterozoic ophiolites (Sichuan, China), and its geotectonic implications: Minerals and Rocks, v. 14, p. 1–15 (in Chinese).

Sun, C. M., and Vuagnat, M., 1992, Proterozoic ophiolites from Yanbian and Shimian (Sichuan Province, China): Petrography, geochemistry, petrogenesis, and geotectonic environment: Schweizerische Mineralogische und Petrographische Mitteilungen, v. 72, p. 389–413.

Sun, S. S., and McDonough, W. F., 1989, Chemical and isotopic systematics of oceanic basalts: Implications for mantle composition and processes, *in* Saunders, A. D., and Norry, M. J., eds. Magmatism in the ocean basins: Geological Society Special Publication, v. 42, p. 313–345.

Wang, J., and Li, Z. X., 2003, History of Neoproterozoic rift basins in South China: Implications for Rodinia break-up: Precambrian Research, v. 122, p. 141–158.

Yan, D. P., Zhou, M. F., Song, H. L., and Nalpas, J., 2002, Where was South China located in the reconstruction of Rodinia?: Earth Science Frontiers, v. 9, p. 49–50 (in Chinese).

Zhong, H., Yao, Y., Hu, S. F., Zhou, X. H., Liu, B. G., Sun, M., Zhou, M. F., and Viljoen, M. J., 2003, Platinum-group element geochemistry of the Hongge Fe-V-Ti deposit in the Pan-Xi area, southwestern China: International Geology Review, v. 45, p. 371–382.

Zhong, H., Yao, Y., Prevec, S. A., Wilson, A. H., Viljoen, M. J., Viljoen, P. R., Liu, B. G., and Luo, Y. N., 2004, Trace-element and Sr-Nd isotopic geochemistry of the PGE-bearing Xiejie layed intrusion in SW China: Chemical Geology, v. 203, p. 237–252.

Zhou, G. Q., and Zhao, J. X., 1991, Sm-Nd isotopic systematics of NE Jiangxi Ophiolite (NEJXO), SE margin of the Yangtze Craton, south China: Chinese Science Bulletin, v. 36, p. 1374–1379.

Zhou, J. C., Wang, X. L., Qiu, J. S., and Gao, J. F., 2004, Chemistry of Meso- and Neoproterozoic mafic-ultramafic rocks from northern Guangxi, China: Arc or plume magmatism?: Geochemical Journal, v. 38, p. 139–152.

Zhou, M. F., Kennedy, A. K., Sun, M., Malpas, J., and Lesher, C. M., 2002a, Neoproterozoic arc-related mafic intrusions along the Northern margin of South China: Implications for the accretion of Rodinia: Journal of Geology, v. 110, p. 611–618.

Zhou, M. F., Yan, D. P., Kennedy, A. K., Li, Y., and Ding, J., 2002b, SHRIMP U-Pb zircon geochronological and geochemical evidence for Neoproterozoic arc-magmatism along the western margin of the Yangtze Block, South China: Earth and Planetary Science Letters, v. 196, p. 51–67.

Zhou, X. M., Zhou, H. B., Yang, J. D., and Wang, J. X., 1989, Sm-Nd isotron age and geological significance of the Fuchuan ophiolite suite, Xi County, Anhui

Province: Chinese Science Bulletin, v. 34, p. 1243–1245 (in Chinese).

Zhu, W. G., 2004, Geochemical characteristics and tectonic setting of Neoproterozoic mafic-ultramafic rocks in the western margin of the Yangtze Craton exampled by the Gaojiacun complex and Lengshuiqing No.101 complex: Unpubl. Ph.D. dissertation, Chinese Academy of Sciences, 125 p. (in Chinese).

Zhu, W. G., Liu, B. G., Deng, H. L., Zhong, H., Li. C. Y., Pi, D. H., Li, Z. D., and Qin, Y., 2004a, Advances in the study of Neoproterozoic mafic-ultramafic rocks on the Western margin of the Yangtze craton: Bulletin of Mineralogy, Petrology, and Geochemistry, v. 23, p. 255–263 (in Chinese).

Zhu, W. G., Zhong, H., Deng, H. L., Liu, B. G., Li, C. Y., and Qin, Y., 2004b, Geochemical characteristics and geochronology of the Lengshuiqing magmatic Cu-Ni sulfide ore deposit in the Yanbian area, Sichuan Province, SW China: Bulletin of Mineralogy, Petrology, and Geochemistry, v. 23 (suppl.), p. 112 (in Chinese).

Zhu, Z. X., 1983, Features and tectonic environments of the Precambrian Yanbian Group volcanic rock series in Sichuan: Minerals and Rocks, v. 3, p. 42–51 (in Chinese).

Zindler, A., and Hart, S. R., 1986, Chemical geodynamics: Annual Review of Earth and Planetary Sciences, v. 14, p. 493–571.